Supporting Information for

From 1D Helix to 0D Loop: Nitrite Anion Induced Structural Transformation Associated with Unexpected Ligand *N*-Nitrosation of Amine Ligand

Jing-Yun Wu,*,† Yu-Chiao Liu‡ and Tzu-Ching Chao†

†Department of Applied Chemistry, National Chi Nan University, Nantou 545, Taiwan. Fax: +886-49-2917956. E-mail: jyunwu@ncnu.edu.tw

‡Institute of Chemistry, Academia Sinica, Taipei 115, Taiwan.

Chart S1 The Two Lewis Resonance Forms of Nitrosamines

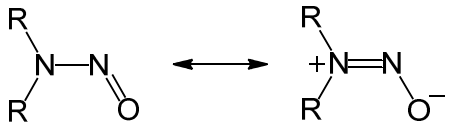

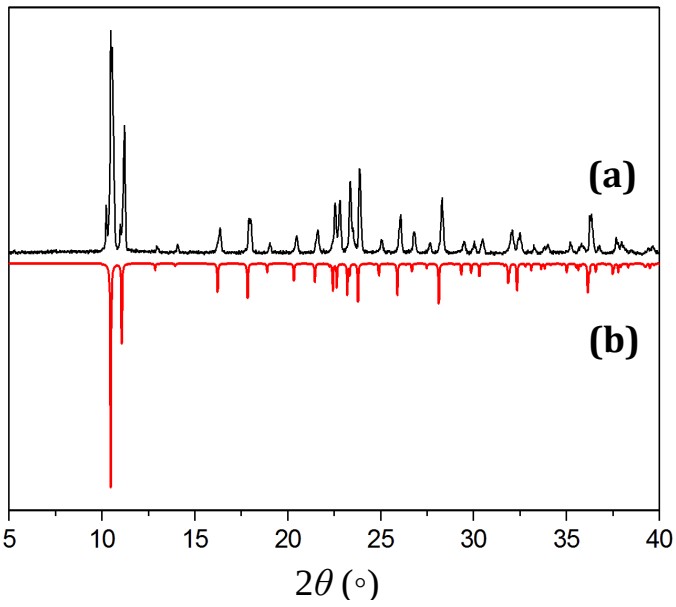

Figure S1. X-ray powder diffraction (XRPD) patterns of **1**: (a) a freshly grounded sample at room temperature; (b) simulated from the single-crystal data.

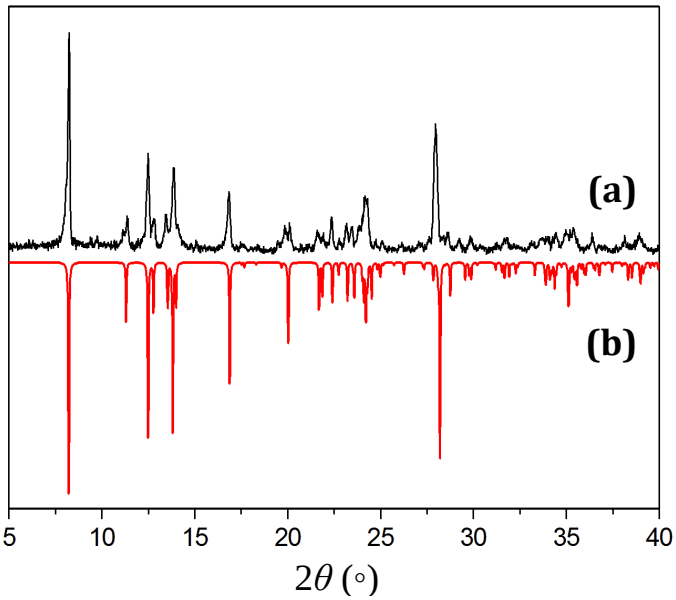

Figure S2. X-ray powder diffraction (XRPD) patterns of **2**: (a) a freshly grounded sample at room temperature; (b) simulated from the single-crystal data.

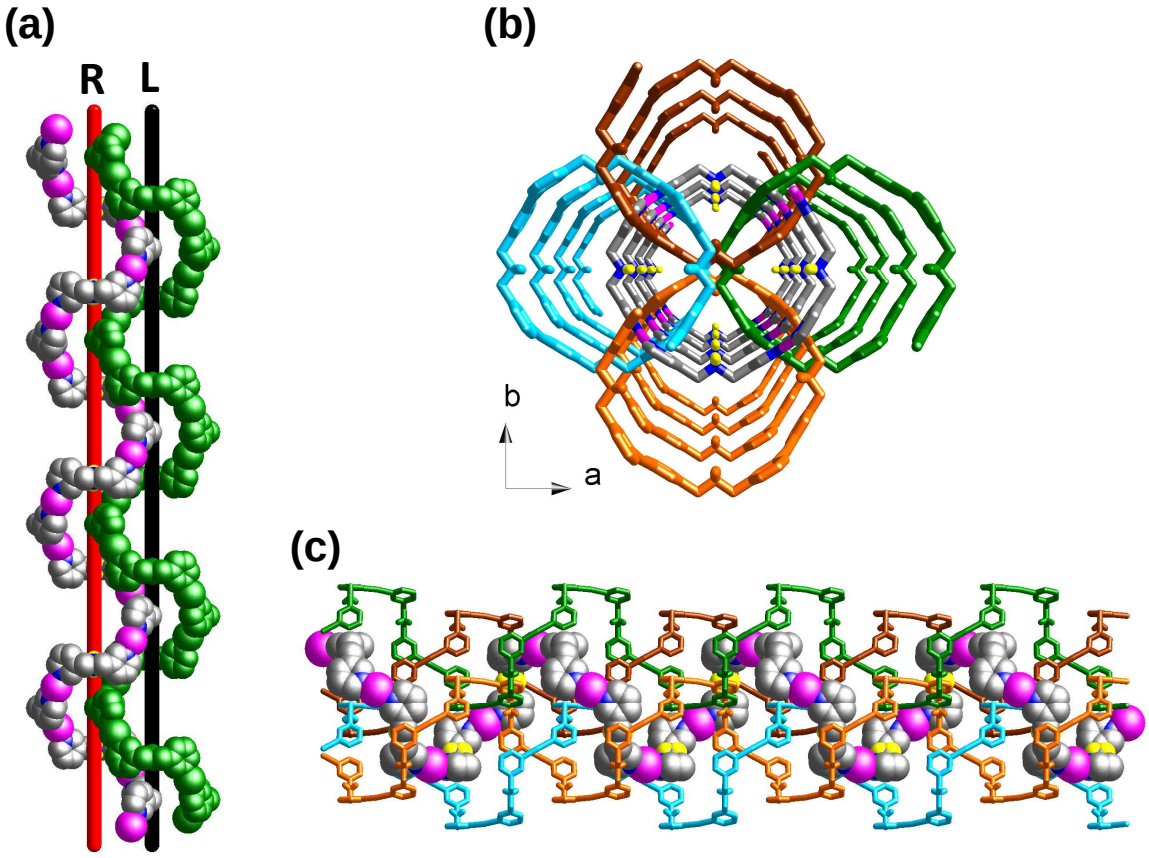

Figure S3. (a) Two opposite-handed 4_1-helices, showing that they are not interweaved with each other. (b) Top- and (c) side-view of the heterochiral 4_1-helices, showing that each 4_1-helix is surrounded by four opposite-handed 4_1-helical chains.

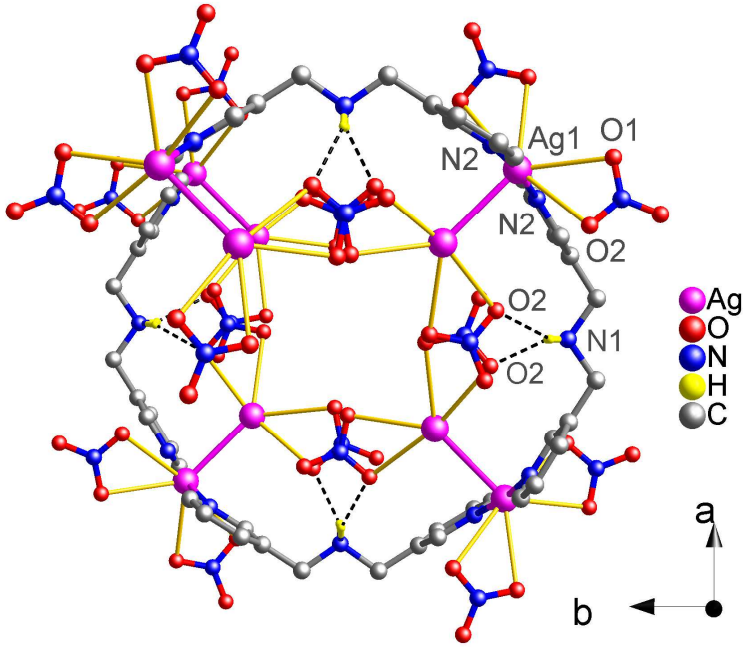

Figure S4. A single 4_1-helix chain structure of **1**, showing weak Ag···O_3N interactions (yellow lines; Ag1–O1, 2.92 Å and Ag1–O2, 2.95 Å), hydrogen-bonding interactions (black dashed lines; N1–H···O2, 2.992(6) Å), and intermolecular argentop hilic interactions (pink lines; 3.0679(6) Å).

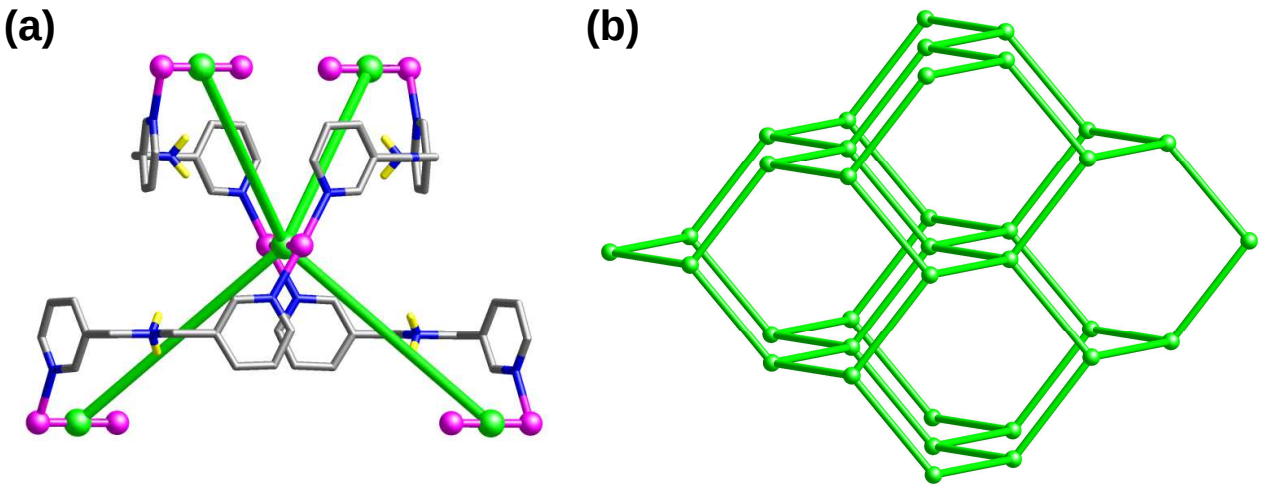

Figure S5. (a) The dinuclear $Ag_2(Hdpma)_4$ secondary building units in **1**, showing the Ag_2 units as tetrahedral junctions (green balls) and the Hdpma ligands as linear linkers (green lines). Color scheme: pink, Ag; blue, N; gray, C; yellow, H. (b) Topological view of a single diamondoid-like net in **1**.

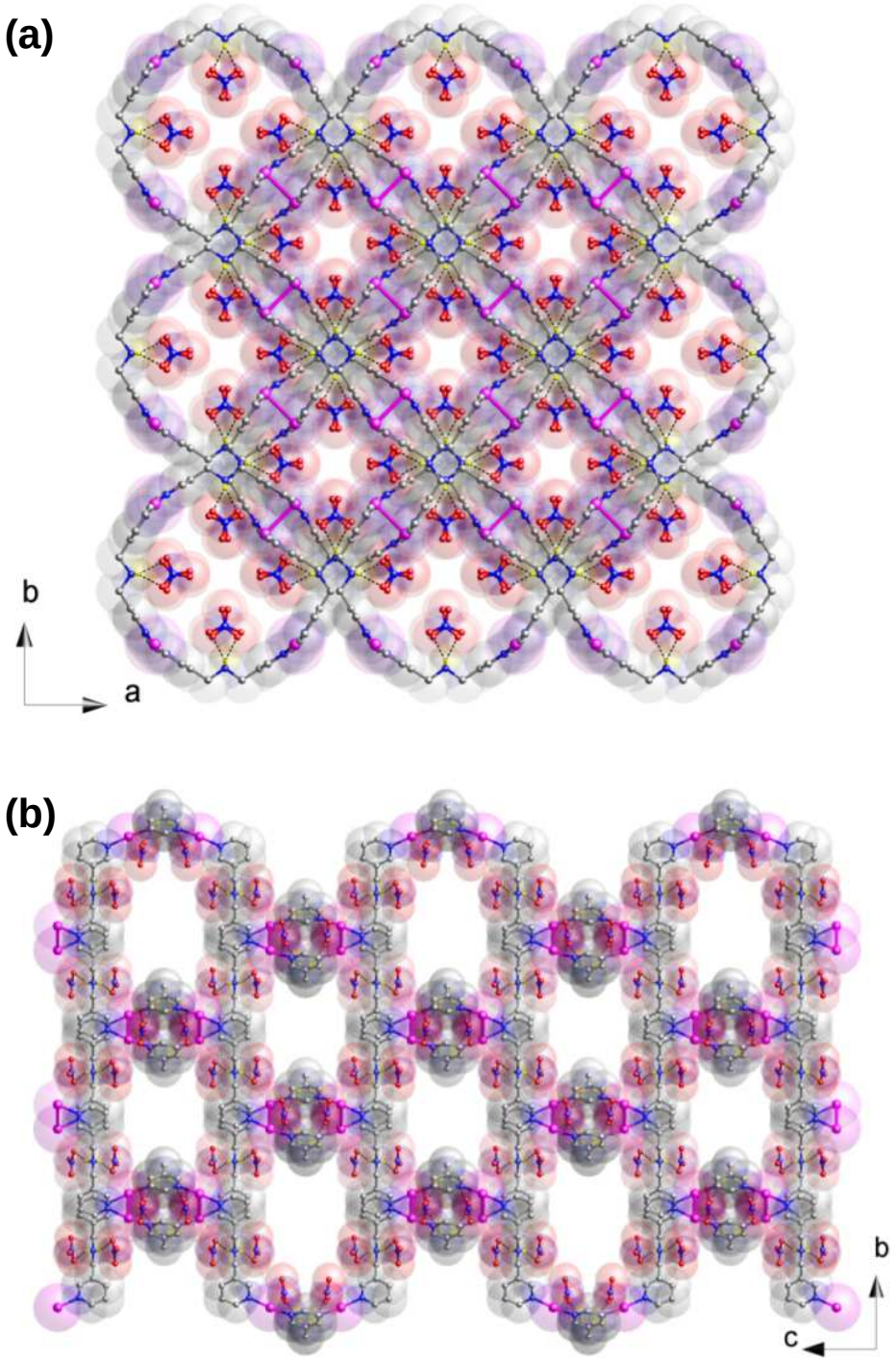

Figure S6. A single network structure of **1** viewed down the crystallographic (a) *c* and (b) *a* axes, showing one-dimensional open channels. Color scheme: pink, Ag; red, O; blue, N; gray, C; yellow, H.

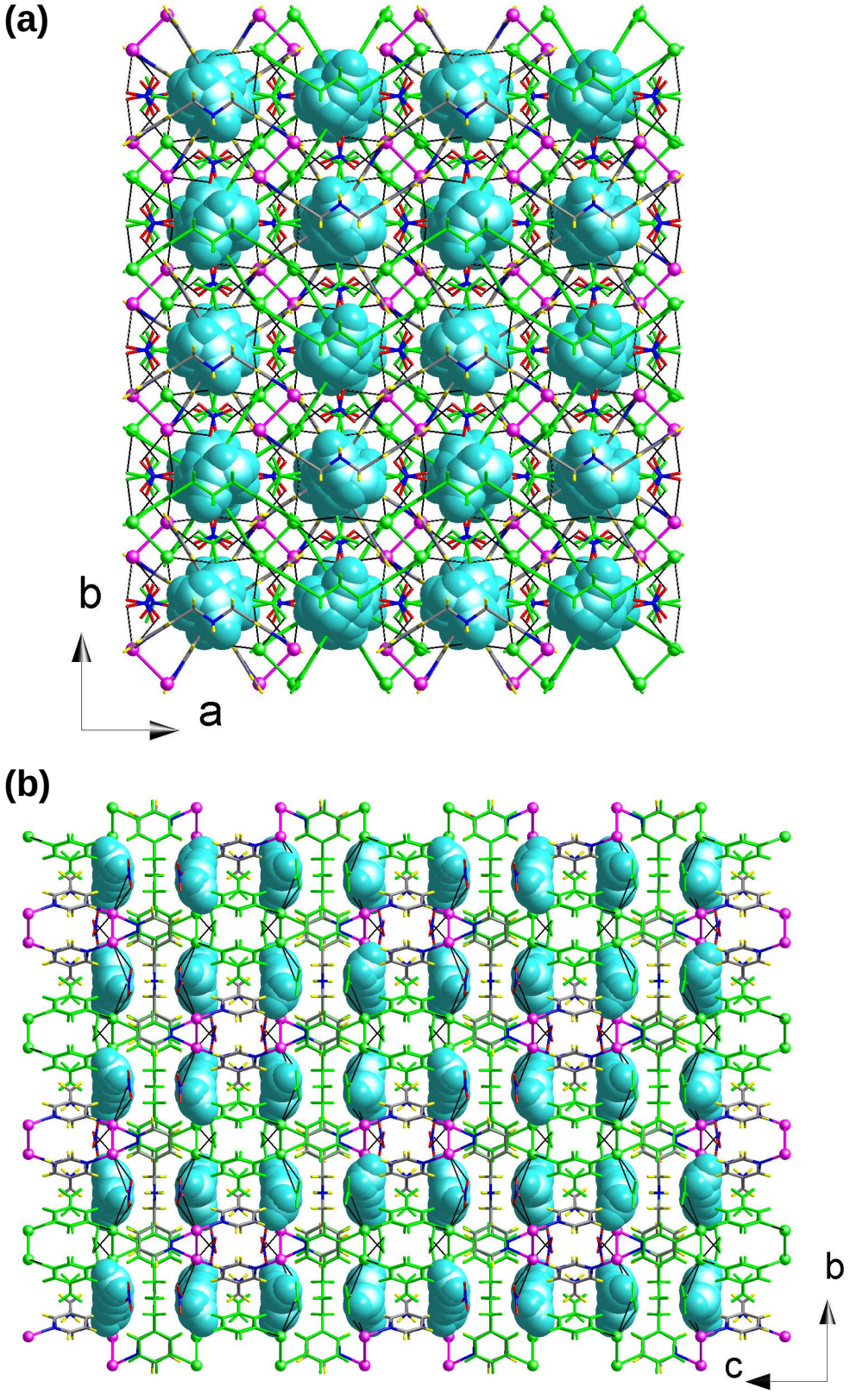

Figure S7. Packing diagrams of **1** viewed down the crystallographic (a) *c* and (b) *a* axes, showing the two-fold interpenetrating nets of opposite-chiralities, each of which consists of five-fold interweaved homochiral 4_1-helical chains locked by ligand-unsupported argentophilic interactions, and lattice water molecules (space-filling model) resided the inter-net void spaces. Color scheme: pink, Ag; red, O; blue, N; gray, C; yellow, H.

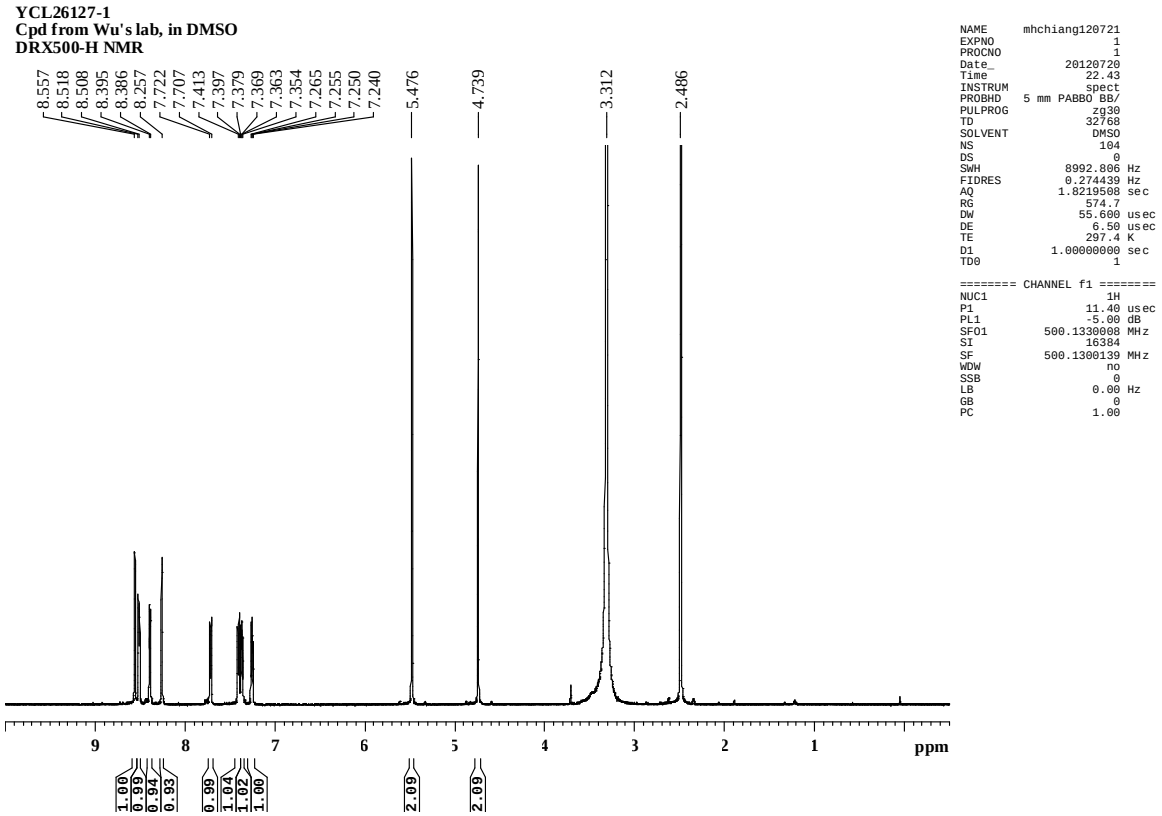

Figure S8. ^{1}H NMR spectrum of molecular loop **2** in DMSO-d_6 at room temperature.

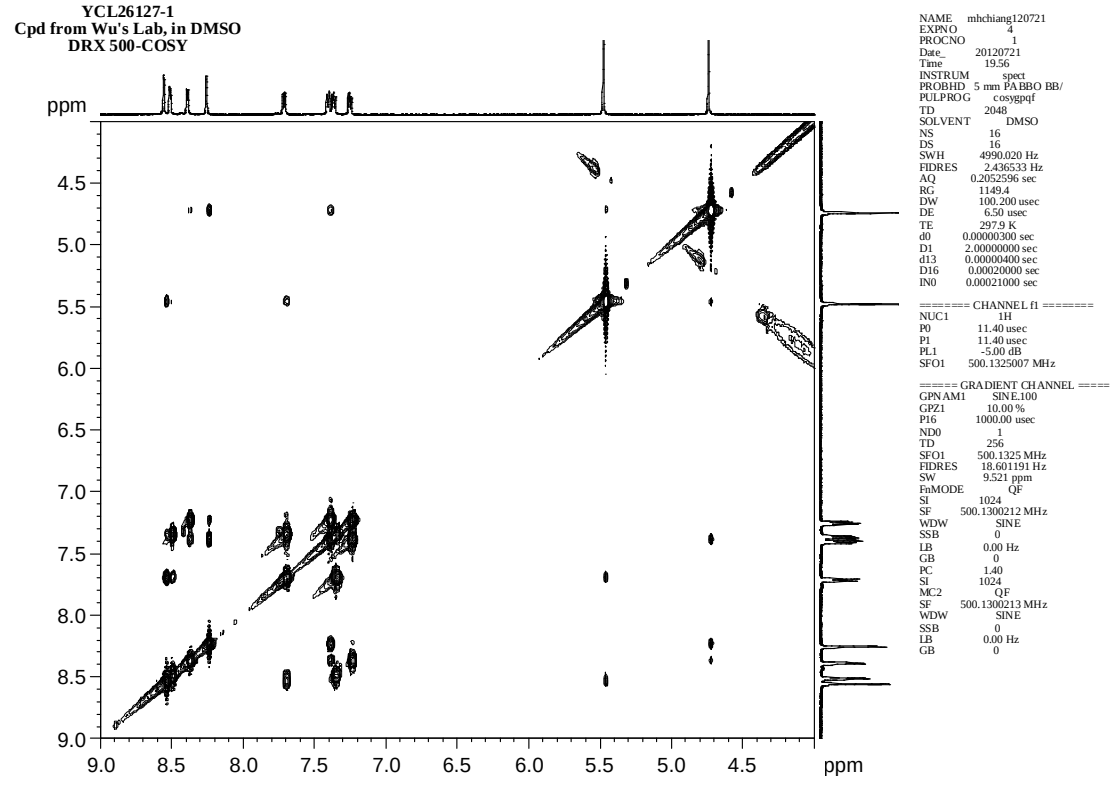

Figure S9. ^{1}H-^{1}H COSY NMR spectrum of molecular loop **2** in DMSO-d_6 at room temperature.

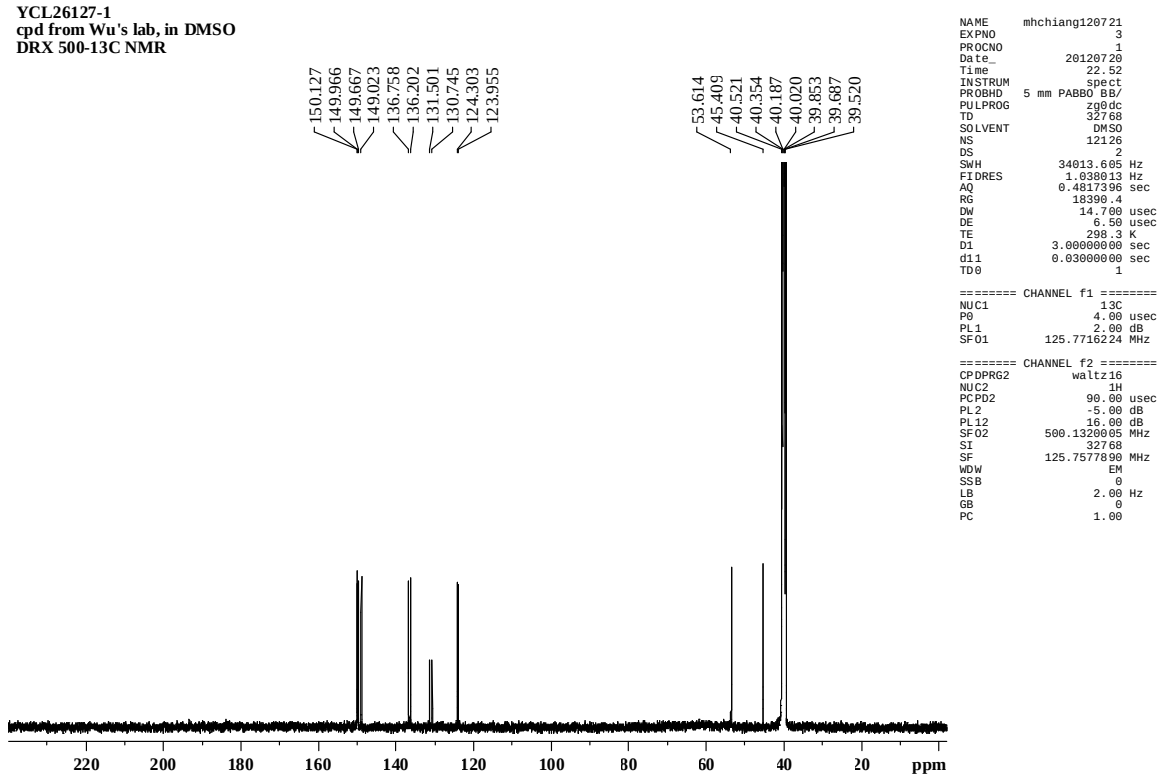

Figure S10. $^{13}C\{^{1}H\}$ NMR spectrum of molecular loop **2** in DMSO-d_6 at room temperature.

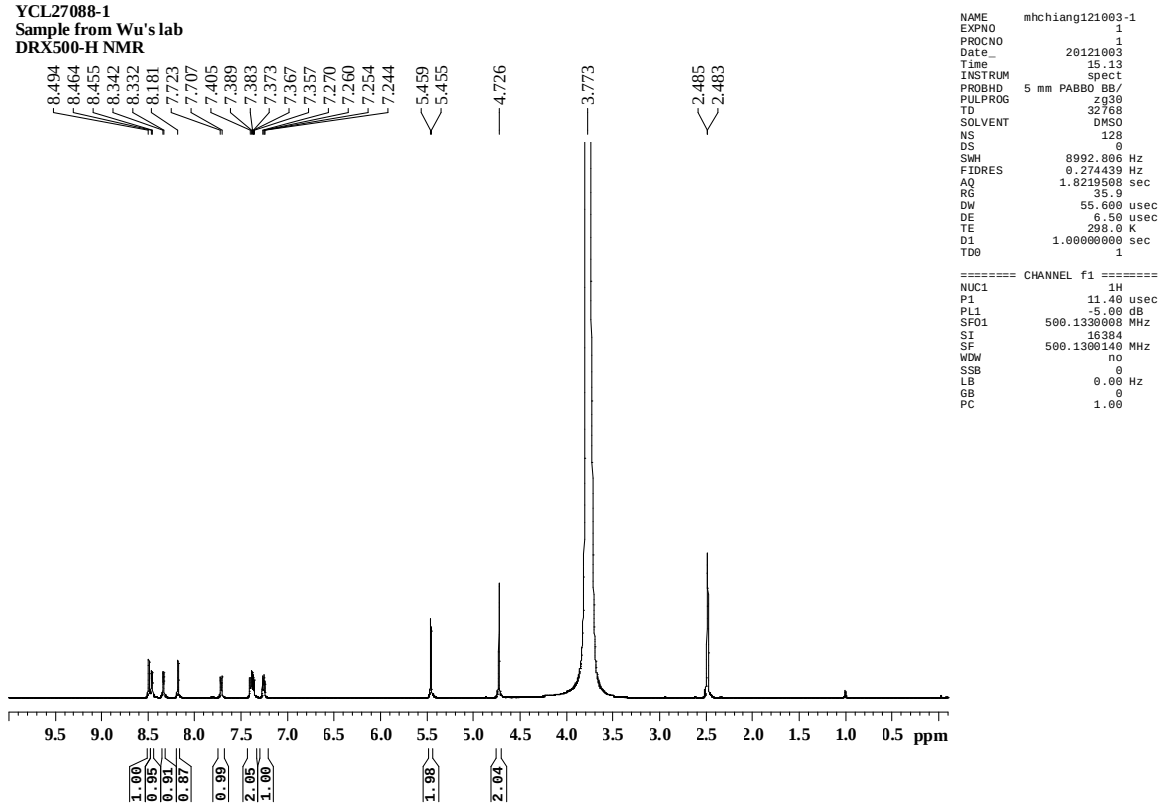

Figure S11. ^{1}H NMR spectrum of ^{15}N-labeled *N*-nitroso molecular loop **2′** in DMSO-d_6 at room temperature.

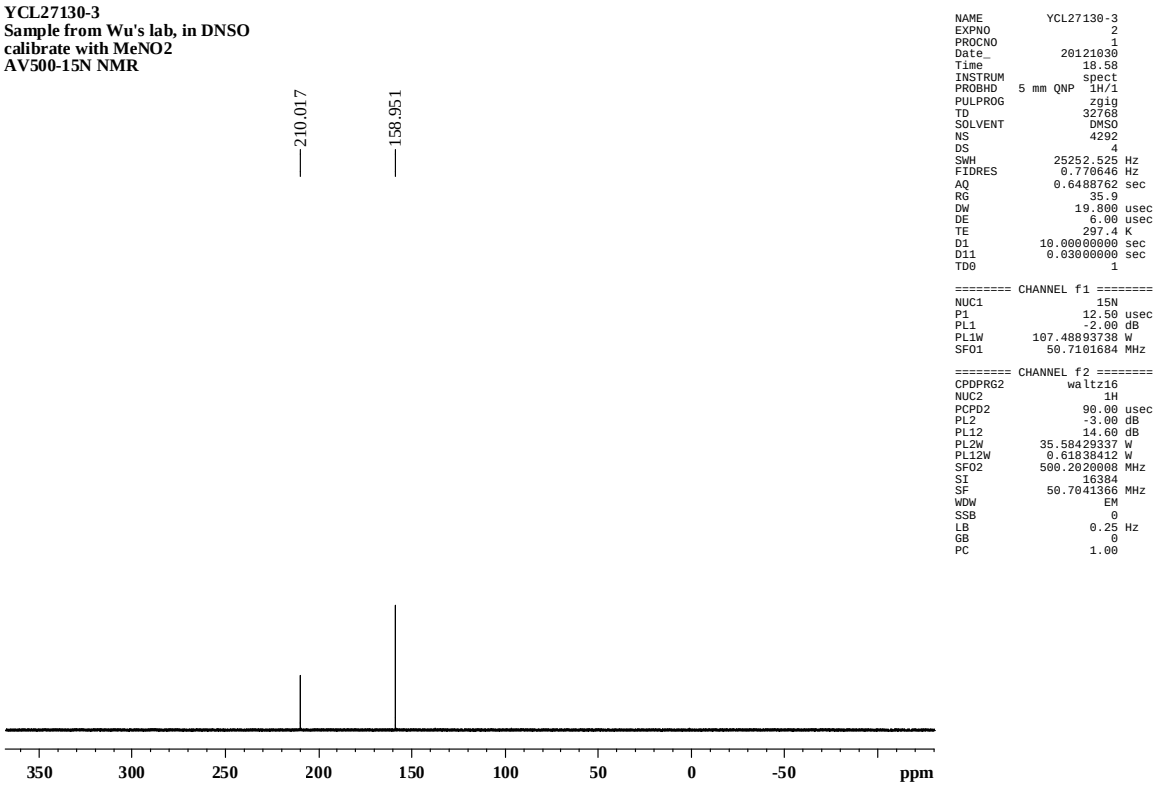

Figure S12. $^{15}N\{^{1}H\}$ NMR spectrum of ^{15}N-labeled *N*-nitroso molecular loop **2′** in DMSO-d_6 at room temperature, with referenced to external nitromethane (= 0 ppm).

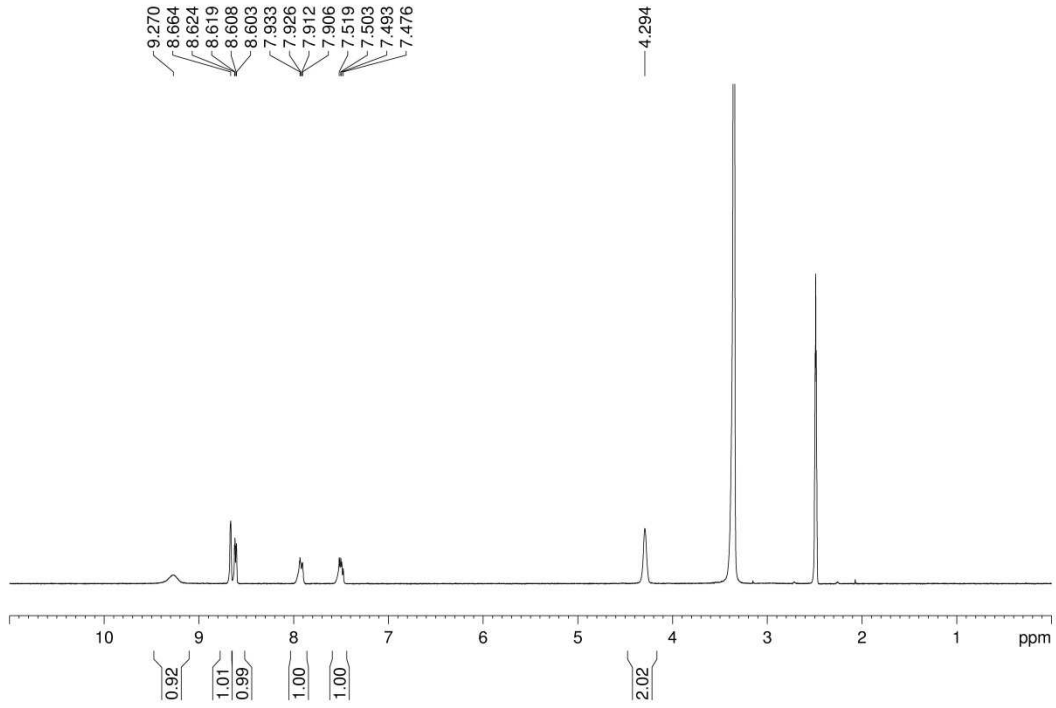

Figure S13. ^{1}H NMR spectrum of helix **1** immersed in DMSO-d_6 at room temperature for 1 day.

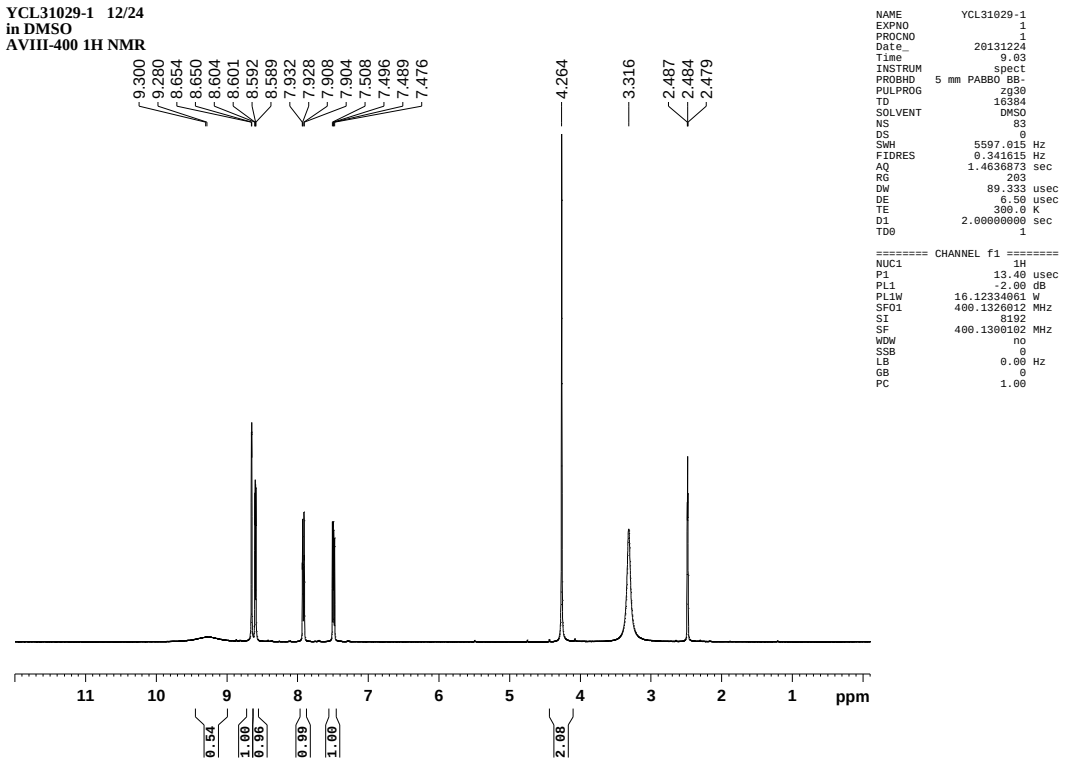

Figure S14. ^{1}H NMR spectrum (DMSO-d_6) of the powdered samples (intermediate ***I***) of immersed **1** in $NaNO_2$ aqueous solution at room temperature after 3 hours.

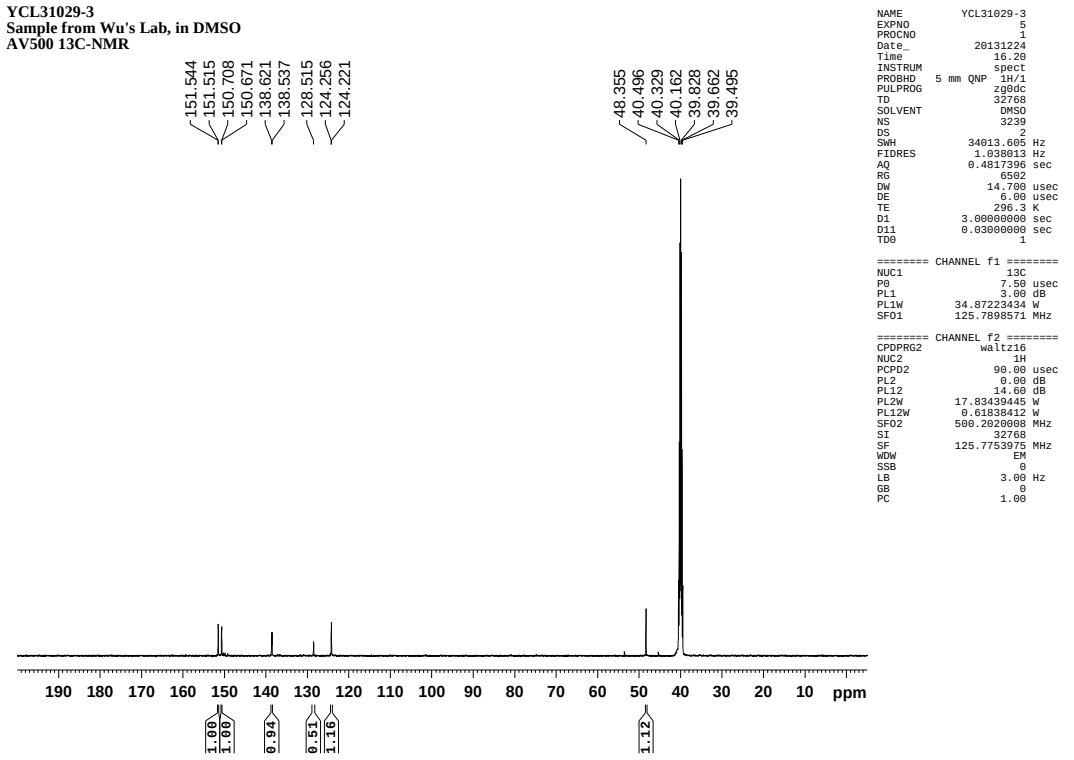

Figure S15. ^{13}C{^{1}H} NMR spectrum (DMSO-d_6) of the powdered samples (intermediate ***I***) of immersed **1** in $NaNO_2$ aqueous solution at room temperature after 3 hours.

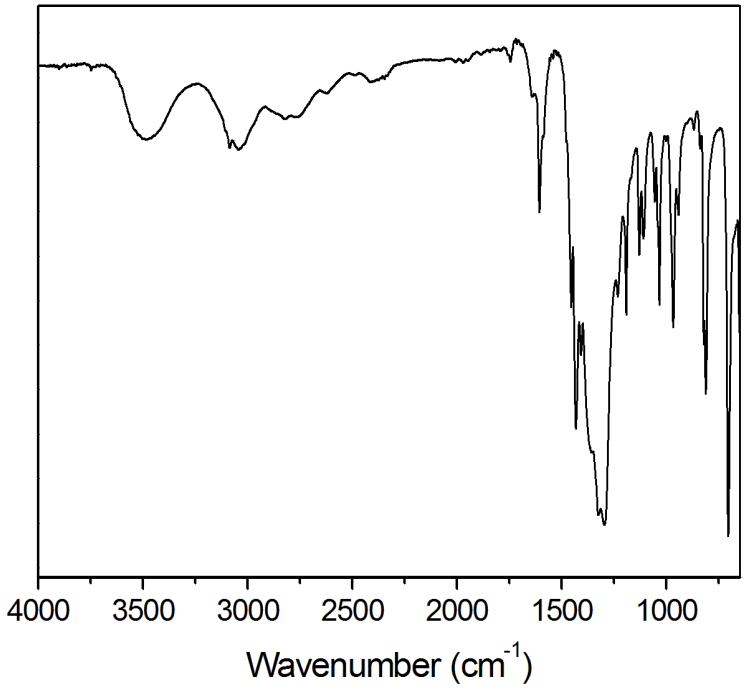

Figure S16. Solid-state IR spectrum of helix **1**.

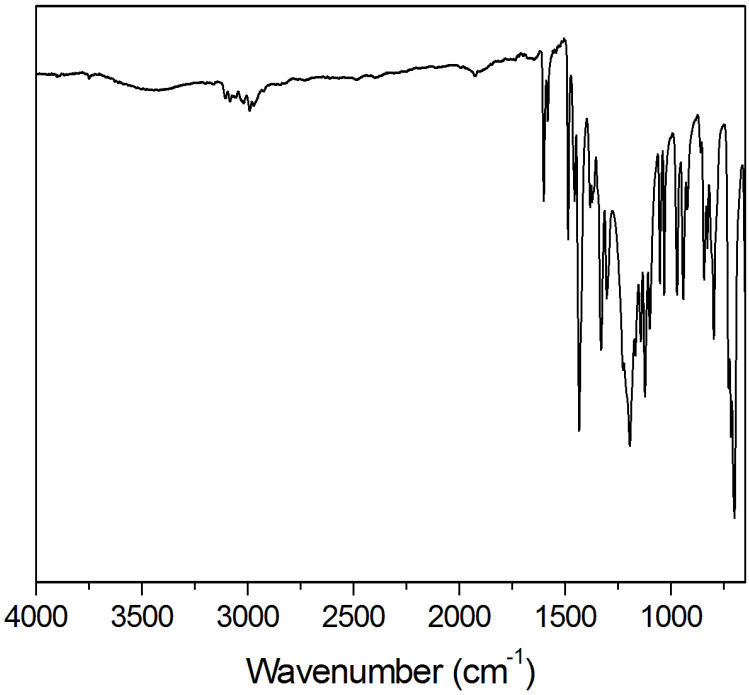

Figure S17. Solid-state IR spectrum of molecular loop **2**.

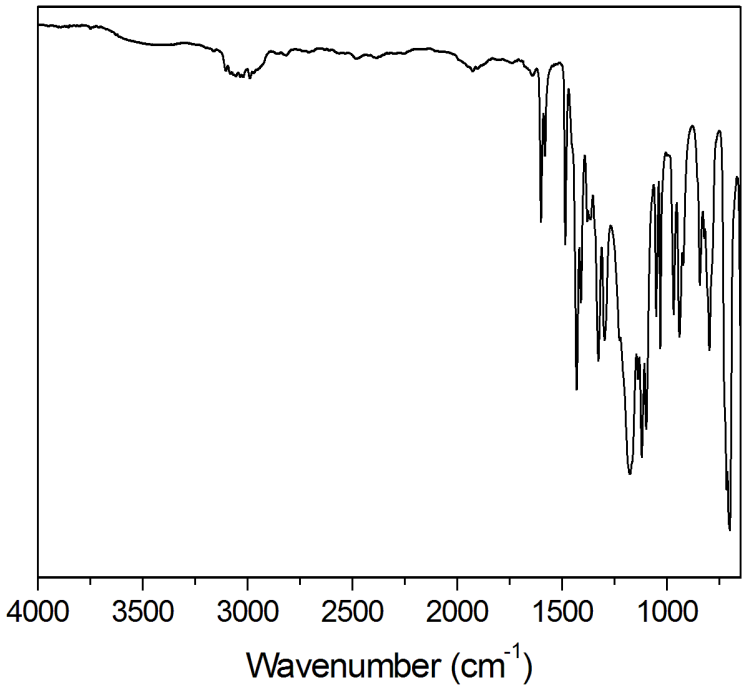

Figure S18. Solid-state IR spectrum of ^{15}N-labeled *N*-nitroso molecular loop **2′**.

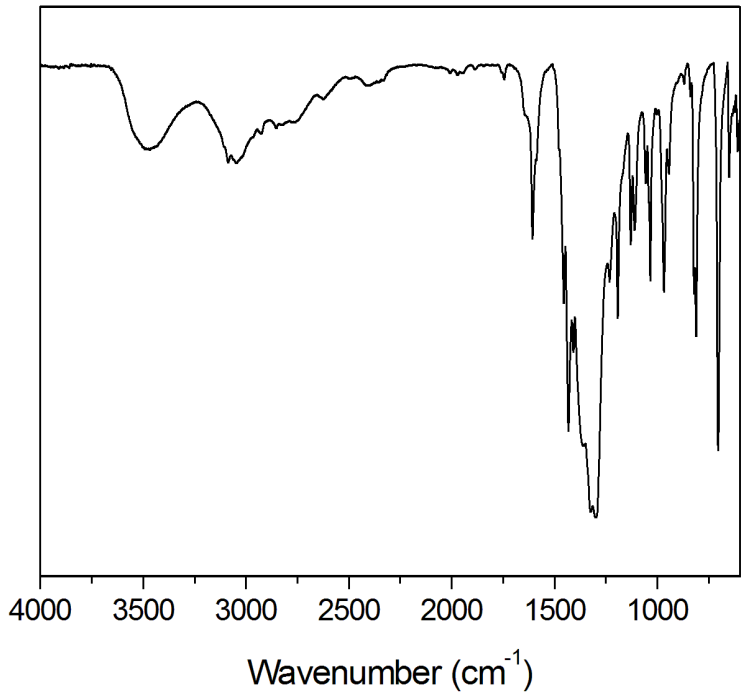

Figure S19. Solid-state IR spectrum of the powdered samples (intermediate ***I***) of immersed **1** in $NaNO_2$ aqueous solution at room temperature for 3 hours.

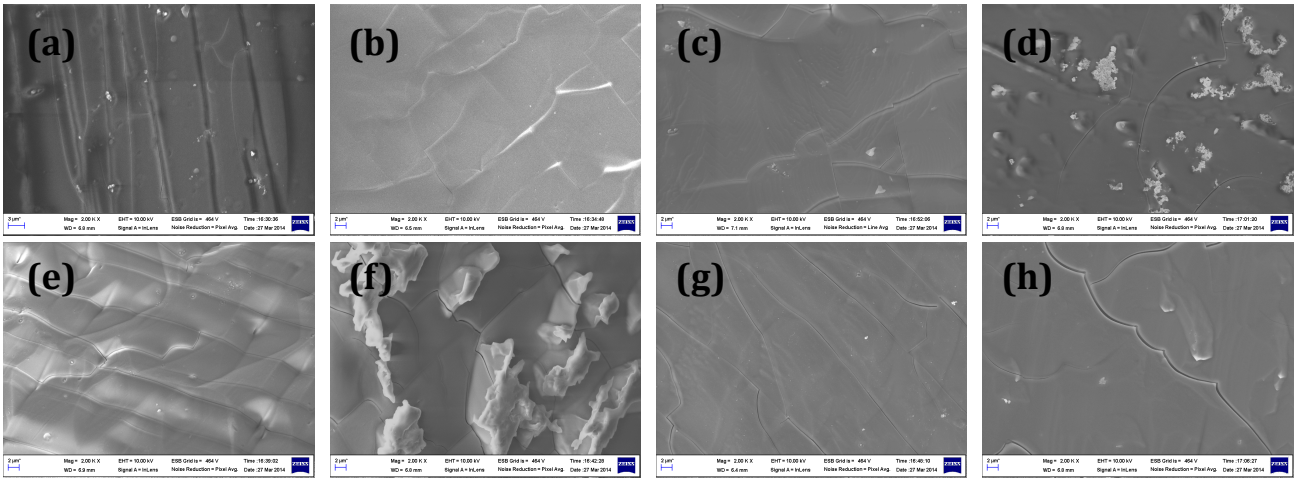

Figure S20. SEM images of crystals of helix **1** (a) before and (b–g) after anion exchange by immersion in an aqueous solution of $NaNO_2$ at room temperature for 5 min, 8 h, 20 h, 3 d, 4 d and 6 d, and (h) of crystal of molecular loop **2**.

(a)

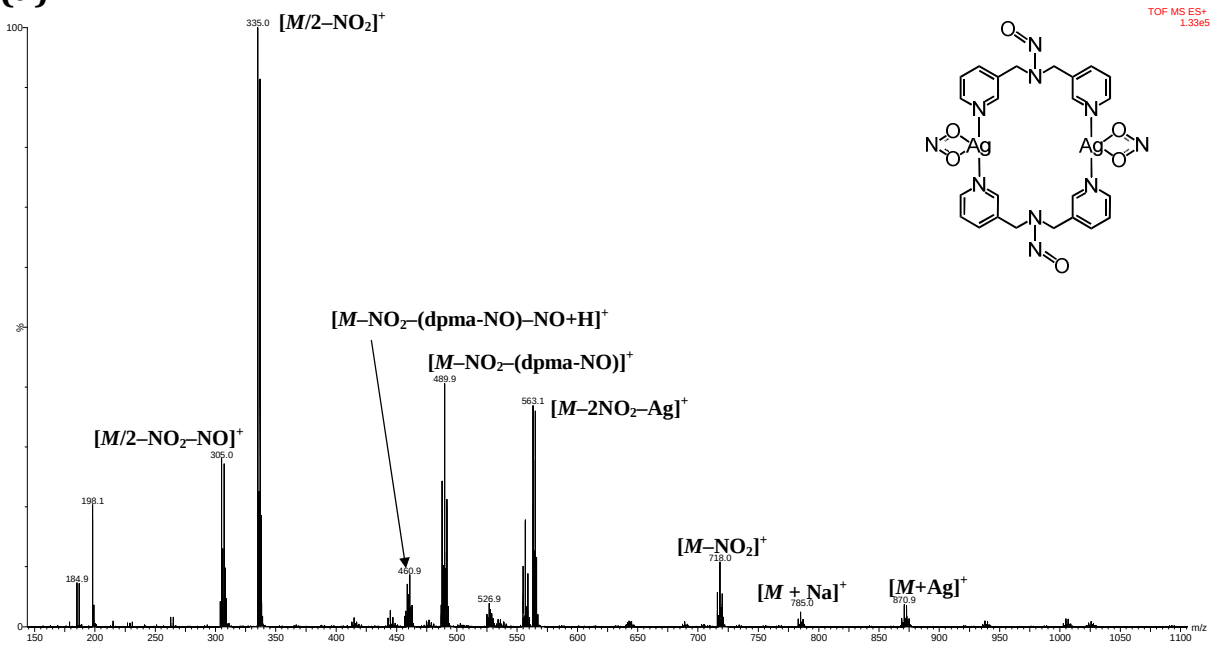

Peaks (m/z)	Assigned fragments	Composition	Calcd value (m/z)
870.9	$[M+Ag]^+$	$[C_{24}H_{24}N_{10}O_6Ag_3]^+$	870.9
785.0	$[M+Na]^+$	$[C_{24}H_{24}N_{10}O_6Ag_2Na]^+$	787.0
718.0	$[M-NO_2]^+$	$[C_{24}H_{24}N_9O_4Ag_2]^+$	718.0
563.1	$[M-2NO_2-Ag]^+$	$[C_{24}H_{24}N_8O_2Ag]^+$	563.1
489.9	$[M-NO_2-(dpma\text{-}NO)]^+$	$[C_{12}H_{12}N_5O_3Ag_2]^+$	489.9
460.9	$[M-NO_2-(dpma\text{-}NO)-NO+H]^+$	$[C_{12}H_{13}N_4O_2Ag_2]^+$	460.9
335.0	$[M/2-NO_2]^+$	$[C_{12}H_{12}N_4OAg]^+$	335.0
305.0	$[M/2-NO_2-NO]^+$	$[C_{12}H_{12}N_3Ag]^+$	305.0

(b) **$[M+Ag]^+$ = $[Ag_3(dpma\text{-}NO)_2(NO_2)_2]^+$** **$[M-NO_2]^+$ = $[Ag_2(dpma\text{-}NO)_2(NO_2)]^+$**

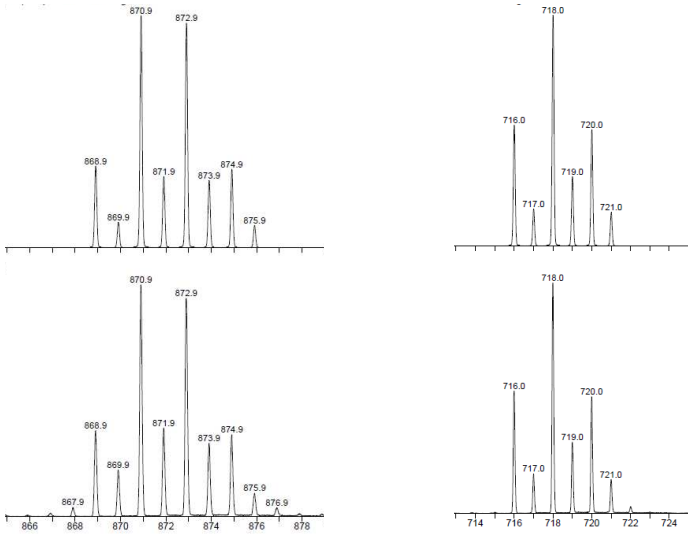

Figure S21. (a) ESI mass spectra of molecular loop **2** in DMSO, along with peak assignments. (b) Theorical (top) and experimental (bottom) isotopic distribution patterns of fragments $[M+Ag]^+$ ($[Ag_3(dpma\text{-}NO)_2(NO_2)_2]^+$, m/z = 870.9, left) and $[M-NO_2]^+$ ($[Ag_2(dpma\text{-}NO)_2(NO_2)]^+$, m/z = 718.0, right), where M = $[Ag(dpma\text{-}NO)(NO_2)]_2$ = $C_{24}H_{24}(^{14}N)_{10}O_6Ag_2$ = 764.0.

(a)

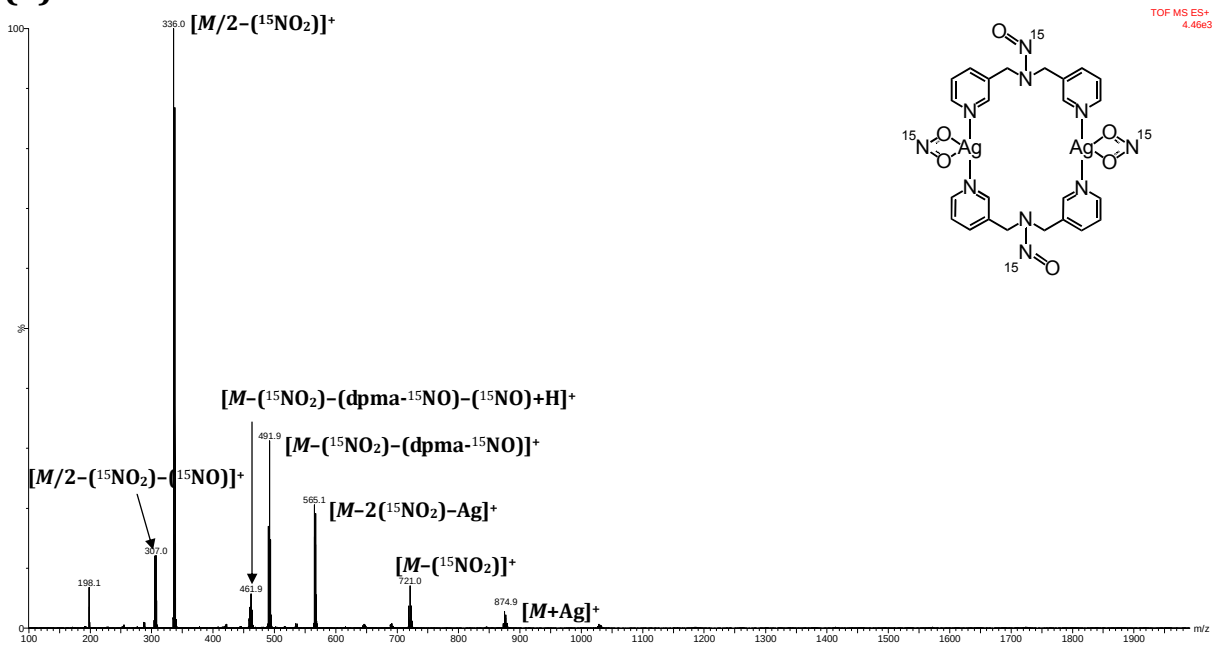

Peaks (m/z)	Assigned fragments	Composition	Calcd value (m/z)
874.9	$[M+Ag]^+$	$[C_{24}H_{24}(^{14}N)_6(^{15}N)_4O_6Ag_3]^+$	874.9
721.0	$[M–(^{15}NO_2)]^+$	$[C_{24}H_{24}(^{14}N)_6(^{15}N)_3O_4Ag_2]^+$	721.0
565.1	$[M–2(^{15}NO_2)–Ag]^+$	$[C_{24}H_{24}(^{14}N)_6(^{15}N)_2O_2Ag]^+$	565.1
491.9	$[M–(^{15}NO_2)–(dpma\text{-}^{15}NO)]^+$	$[C_{12}H_{12}(^{14}N)_6(^{15}N)_2O_3Ag_2]^+$	491.9
461.9	$[M–(^{15}NO_2)–(dpma\text{-}^{15}NO)–(^{15}NO)+H]^+$	$[C_{12}H_{13}(^{14}N)_6(^{15}N)_1O_2Ag_2]^+$	461.9
336.0	$[M/2–(^{15}NO_2)]^+$	$[C_{12}H_{12}(^{14}N)_3(^{15}N)_1OAg]^+$	336.0
307.0	$[M/2–(^{15}NO_2)–(^{15}NO)]^+$	$[C_{12}H_{12}(^{14}N)_3Ag]^+$	305.0

(b) **$[M+Ag]^+$ = $[Ag_3(dpma\text{-}^{15}NO)_2(^{15}NO_2)_2]^+$**

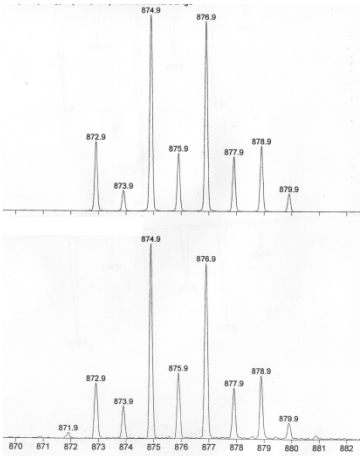

$[M–NO_2]^+$ = $[Ag_2(dpma\text{-}^{15}NO)_2(^{15}NO_2)]^+$

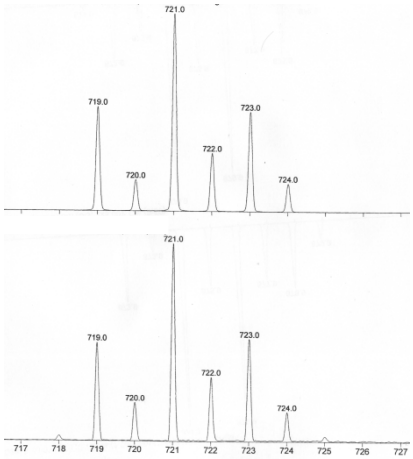

Figure S22. (a) ESI mass spectra of ^{15}N-labeled *N*-nitroso molecular loop **2′** in DMSO, along with peak assignments. (b) Theorical (top) and experimental (bottom) isotopic distribution patterns of fragments $[M+Ag]^+$ ($[Ag_3(dpma\text{-}^{15}NO)_2(^{15}NO_2)_2]^+$, m/z = 874.9, left) and $[M–NO_3]^+$ ($[Ag_2(dpma\text{-}^{15}NO)_2(^{15}NO_2)]^+$, m/z = 721.0, right), where M = $[Ag(dpma\text{-}^{15}NO)(^{15}NO_2)]_2$ = $C_{24}H_{24}(^{14}N)_6(^{15}N)_4O_6Ag_2$ = 768.0

(a)

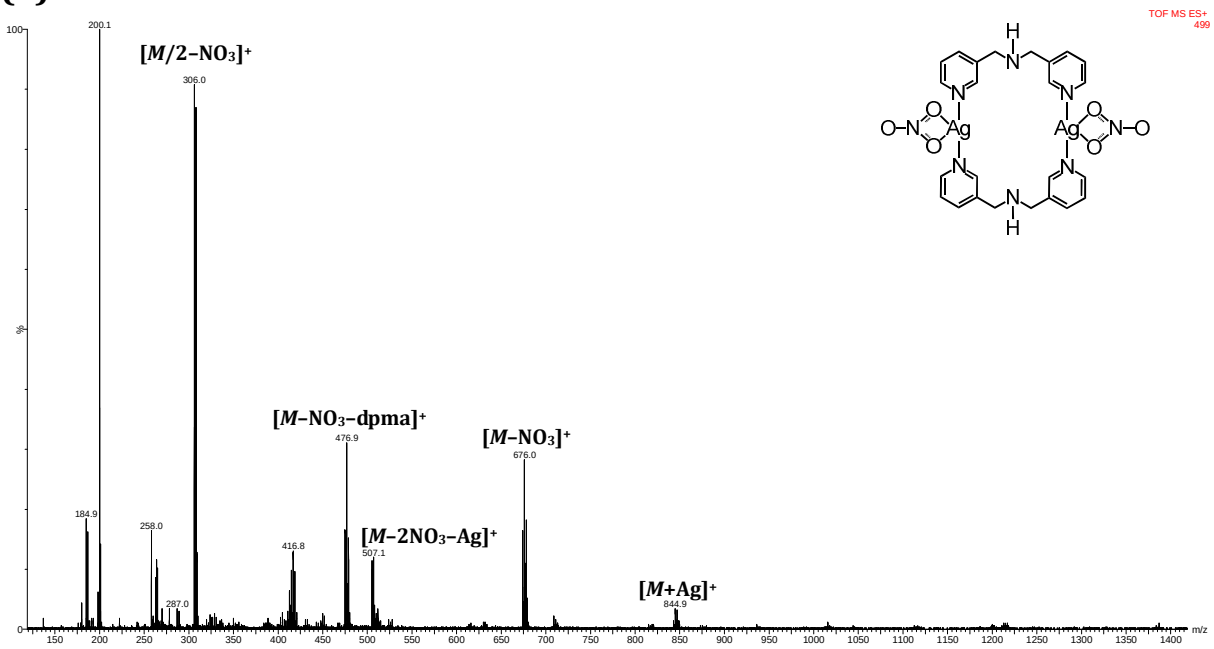

Peaks (m/z)	Assigned fragments	Composition	Calcd value (m/z)
844.9	$[M+Ag]^+$	$[C_{24}H_{26}N_8O_6Ag_3]^+$	844.9
676.0	$[M-NO_3]^+$	$[C_{24}H_{26}N_7O_3Ag_2]^+$	676.0
507.1	$[M-2NO_3-Ag]^+$	$[C_{24}H_{24}N_6Ag]^+$	505.1
476.9	$[M-NO_3-dpma]^+$	$[C_{12}H_{13}N_4O_3Ag_2]^+$	476.9
306.0	$[M/2-NO_3]^+$	$[C_{12}H_{13}N_3Ag]^+$	306.0

(b) **$[M+Ag]^+$ = $[Ag_3(dpma)_2(NO_2)_3]^+$** **$[M-NO_2]^+$ = $[Ag_2(dpma)_2(NO_3)]^+$**

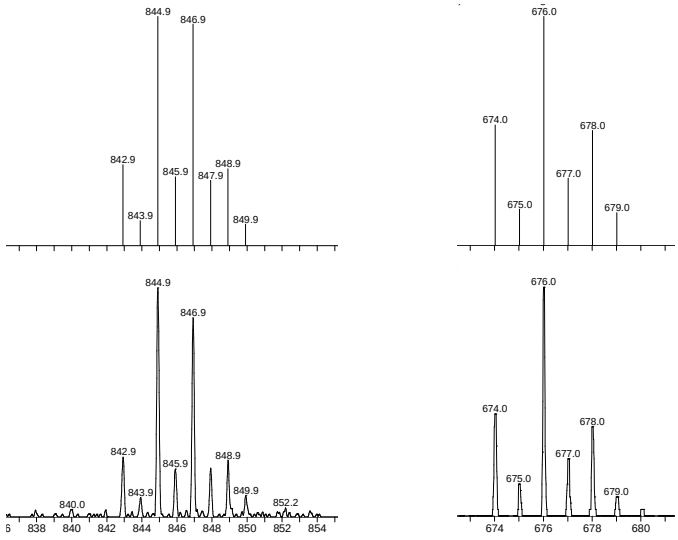

Figure S23. (a) ESI mass spectra (in DMSO) of the powdered samples (intermediate ***I***) of immersed **1** in $NaNO_2$ aqueous solution at room temperature for 3 hours, along with peak assignments. (b) Theorical (top) and experimental (bottom) isotopic distribution patterns of fragments $[M+Ag]^+$ ($[Ag_3(dpma)_2(NO_3)_2]^+$, m/z = 844.9, left) and $[M-NO_3]^+$ ($[Ag_2(dpma)_2(NO_3)]^+$, m/z = 676.0, right), where M = $[Ag(dpma)(NO_3)]_2$ = $C_{24}H_{26}N_8O_6Ag_2$ = 738.0.

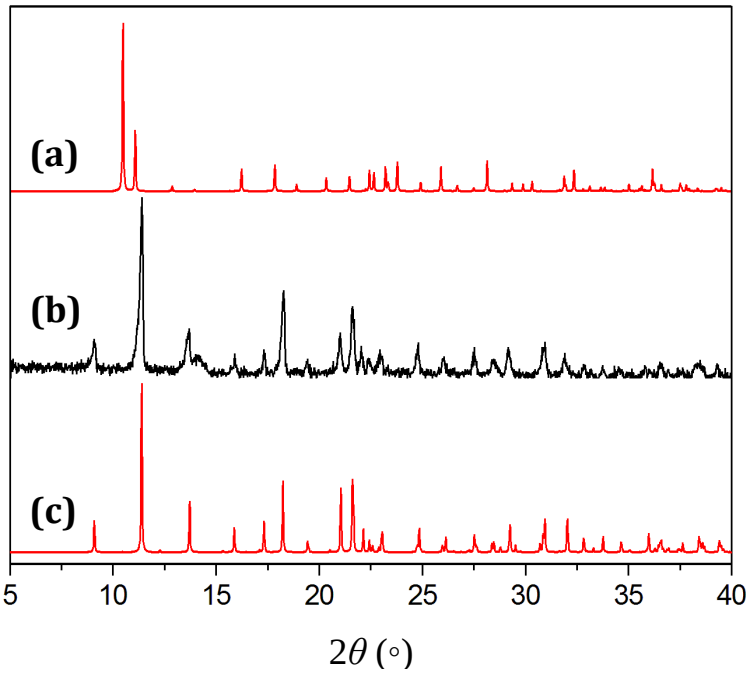

(d)

	crystal sample obtained from **1**/TBAF(aq)	[Ag(dpma)(H_2O)](NO_3)
a (Å)	10.1154(3)	10.1561(12)
b (Å)	12.8367(3)	12.9047(16)
c (Å)	11.6197(4)	11.6393(14)
β (deg)	107.011(3)	106.807(5)
V (Å^3)	1442.79(7)	1460.3(3)

(e)

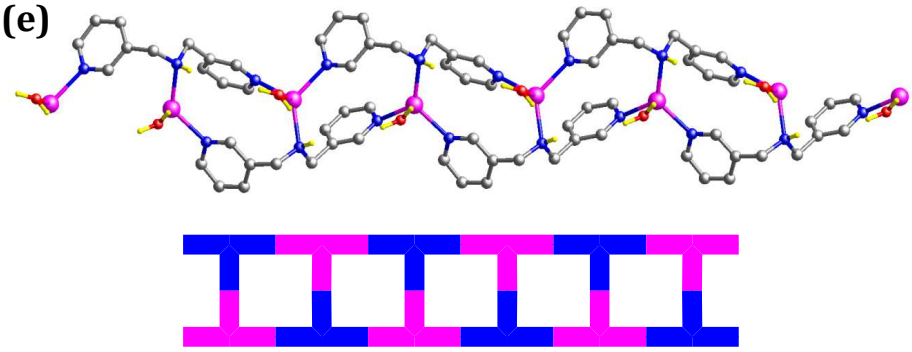

Figure S24. (a) Simulated XRPD pattern of helix **1**. (b) Experimental XRPD pattern of the powdered samples of helix **1** immersed in an aqueous solution of TBAF. (c) Simulated XRPD pattern of [Ag(dpma)(H_2O)](NO_3) (ref 18). (d) Comparison of unit cell parameters between crystal samples obtained from an aqueous solution of **1**/TBAF and [Ag(dpma)(H_2O)](NO_3). (e) Perspective and topologic views of the one-dimensional Ag–dpma binodal ladder-like chain structure including coordinated aqua ligands in [Ag(dpma)(H_2O)](NO_3). Nitrate counteranions and carbon-bound hydrogen atoms are omitted for clarity.

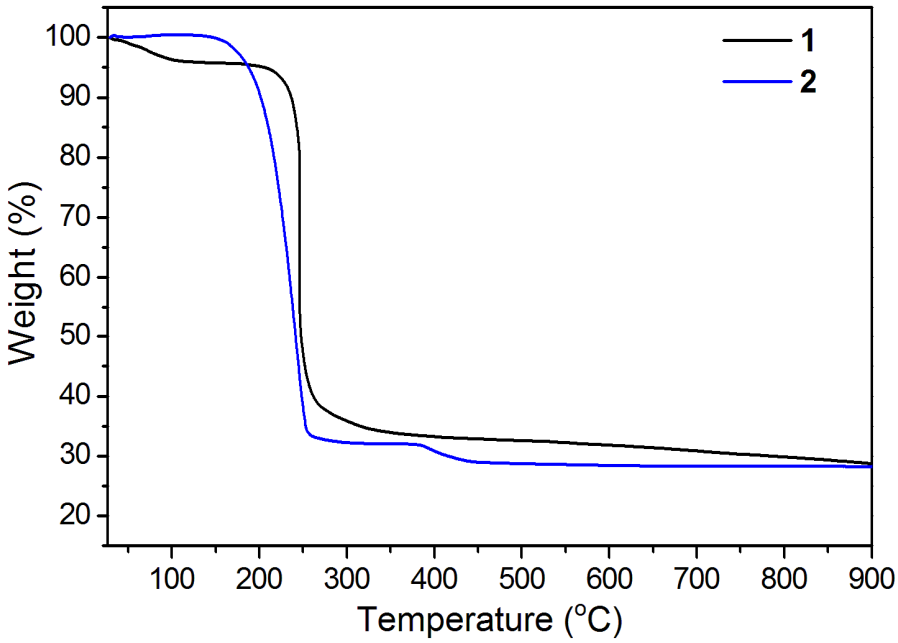

Figure S25. Thermogravimetric (TG) analyses of helix **1** (black) and molecular loop **2** (blue).

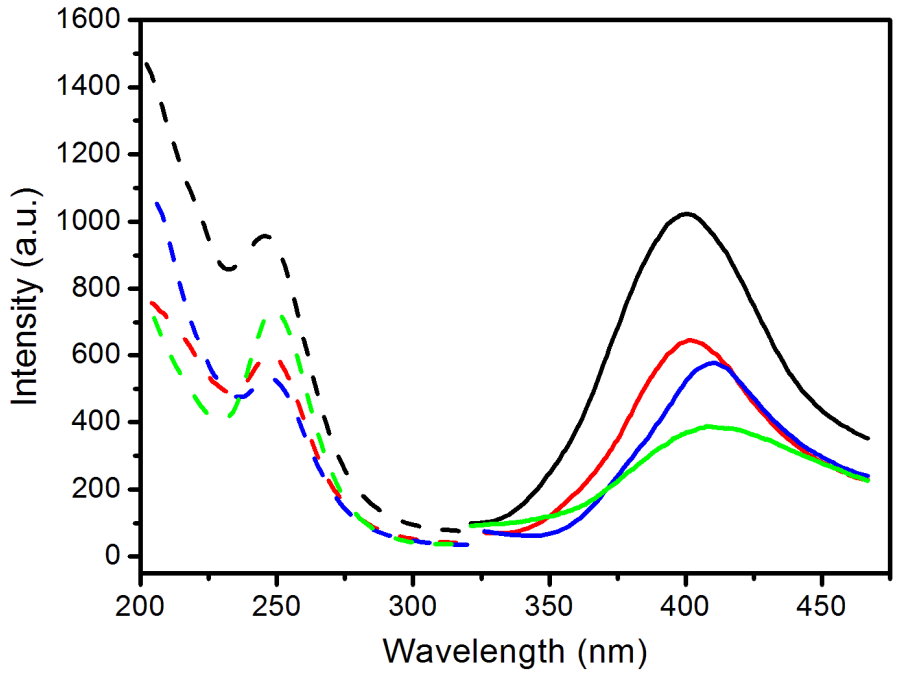

Figure S26. Solid-state excitation (dashed lines, λ_{em} = 400 nm) and emission (solid lines, λ_{ex} = 240 nm) spectra of helix **1** (black), intermediate ***I*** (red), molecular loop **2** (blue), and ladder-like [Ag(dpma)(H_2O)](NO_3) (green) at room temperature. Reproduced with permission from ref 18. Copyright 2013, American Chemical Society.